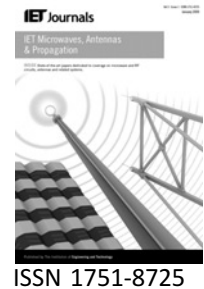


Published in IET Microwaves, Antennas & Propagation
 Received on 27th November 2007
 Revised on 31st August 2008
 doi: 10.1049/iet-map.2008.0130



Broadband millimetre-wave passive spatial combiner based on coaxial waveguide

K. Song^{1,2} Y. Fan¹ X. Zhou²

¹School of Electronic Engineering, University of Electronic Science and Technology of China, Chengdu, Sichuan 610054, People's Republic of China

²Department of Geophysical Engineering, Montana Tech of the University of Montana, Butte MT 59701, USA
 E-mail: kjsong@ee.uestc.edu.cn

Abstract: A broadband millimetre-wave passive spatial combiner using a microstrip probe array and an oversized coaxial waveguide is successfully designed and tested. The equivalent circuit approach of transverse electromagnetic (TEM) lines is adopted to synthesise the coaxial stepped impedance transformer from a K connector with the oversized coaxial waveguide and to analyse the microstrip probe array. The equivalent susceptances of the step discontinuities for the power divider are calculated. A four-way coaxial waveguide passive power combining circuit operating at the entire Ka-band is designed, fabricated and measured. Experiments on the four-way passive combiner show that a minimum insertion loss of 0.7 dB has been achieved at about 29.5 GHz. The combiner has shown a bandwidth of 26.5–40 GHz with 10 dB return loss and less than 2.5 dB insertion loss.

1 Introduction

Millimetre-wave amplifiers with high power and broad bandwidth are difficult to realise in monolithic microwave integrated circuit (MMIC). One way to overcome the technical difficulty is to combine output powers from multiple solid-state devices. Therefore a variety of power dividing and combining techniques, including both resonant structures such as cavity combiners and structures of wider bandwidth such as popular Wilkinson devices, has been developed [1–7].

The spatial power combiner based on a rectangular waveguide has been developed in the past decade [8–12], but the bandwidth of the rectangular waveguide is limited by the cutoff frequency [13–15]. In addition, the dominant TE₁₀ mode inside a rectangular waveguide leads to a non-uniform illumination of the loaded antenna trays inside the waveguide. Besides, the rectangular waveguide environment is dispersive, making it more complicated for the broadband impedance matching over an extended frequency range.

To overcome these difficulties, an oversized coaxial waveguide combiner using a finline array was proposed in

[13–16]. The combiner is fed by gradually flared coaxial lines, tapering to standard coaxial connectors at both ends. This coaxial waveguide combiner has broader frequency characteristics than a rectangular waveguide combiner. However, the topology of a coaxial waveguide combiner involves complex design and is thus hard to fabricate. Also, the heat from MMIC amplifiers cannot be removed efficiently.

In a previous paper, Song *et al.* [17] proposed a Ku-band coaxial waveguide power divider/combiner using coaxial probe array and achieved low-loss coaxial-to-waveguide transitions. Furthermore, the broadband coaxial-to-waveguide transition provides better compatibility with commercial MMIC amplifiers. The electromagnetic modelling of this power dividing/combining structure has been developed. Analysis based on the equivalent circuit method provides the design formula for a perfect power dividing/combining structure. In this paper, we present in detail the development of a millimetre-wave passive spatial combiner using a microstrip probe array in an oversized coaxial waveguide. The combiner is fed by a 50 Ω coaxial line transformer. We use a stepped impedance transformer to provide a smooth impedance transition from the type-K connectors to the oversized coaxial waveguide. Both

simulation and measurement show that a bandwidth of 26.5–40 GHz can be achieved.

2 Analysis and design of an oversized coaxial waveguide combiner

2.1 Structure

Fig. 1 depicts the sketch of an oversized coaxial waveguide combiner including the amplifier connections. The combiner is terminated by type-K connectors available commercially. The input signal is fed to the input of the left oversized coaxial waveguide, and then divided equally into N -way signals using a microstrip probe array, where each is then fed to an amplifier of the coaxial waveguide. The N amplified signals are then collected using a coaxial combiner very similar to the coaxial divider and are output to the K-connector on the right.

2.2 Design of stepped impedance transformer

The combiner is fed by a 50 Ω input coaxial line transformer. We use a stepped impedance transformer to provide a smooth impedance transition from the 50 Ω input coaxial line to the oversized coaxial waveguide. The structure shown in Fig. 2 has two step discontinuities. The equivalent circuit approach is adopted to design this stepped impedance transformer. The first step discontinuity is because of the transition of the characteristic impedance from Z_0 to Z_1 . The structure and equivalent circuit are shown in Fig. 3. It is a junction of two coaxial guides of equal inner but different outer radii.

The parameters of the equivalent circuit at the reference plane T can be expressed as [18]

$$\frac{Y'_0}{Y_0} = \frac{\ln(c/a)}{\ln(b/a)} \quad (1)$$

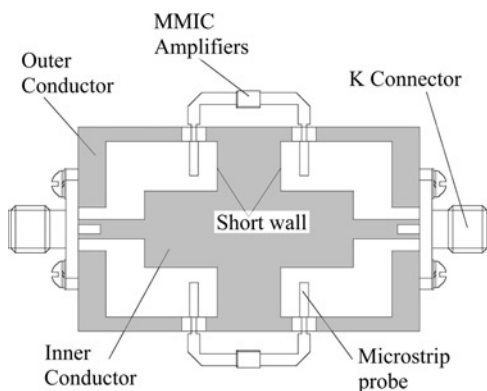


Figure 1 Sketch of an oversized coaxial waveguide combiner

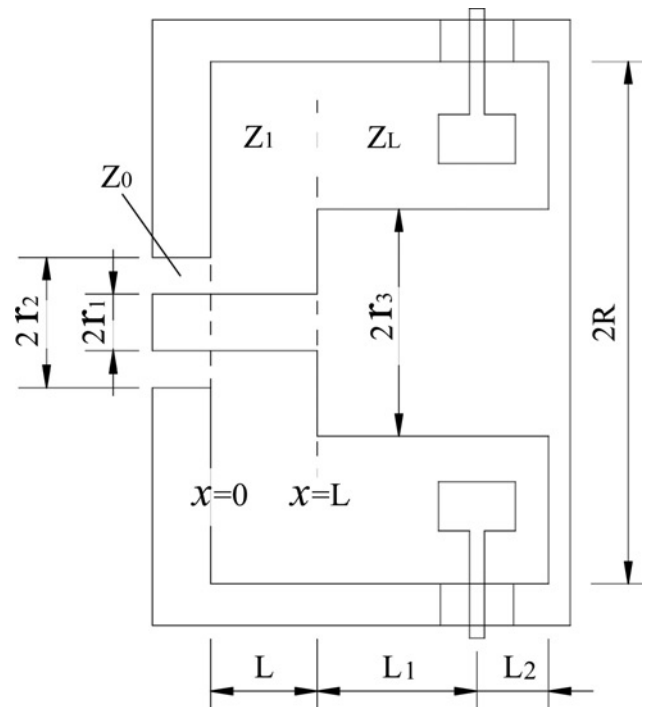


Figure 2 Coaxial stepped impedance transformer circuit

$$\frac{B}{Y_0} = \frac{2b_0 A_1}{\lambda} \left[2 \ln \frac{2.718}{4\alpha} + \frac{2\alpha^2}{3} + 4 \left(\frac{b_0}{\lambda} \right)^2 (1 - \alpha^2)^4 + \frac{A_2}{2} \right] \quad (2)$$

where

$$\alpha = 1 - \delta = \frac{b-a}{c-a}, \quad b_0 = c - a,$$

$$A_1 = \frac{a \ln(c/a)}{b(c/a) - 1} \left[\frac{(b/a) - 1}{\ln(b/a)} \right]^2$$

and

$$A_2 = \frac{\pi^2(c/b)}{\gamma_1 \sqrt{1 - (2b_0/\gamma_1\lambda)^2}} \frac{1 - (a/c)}{1 - [J_0^2(x)/J_0^2(xa/c)]} \times \left[\frac{J_0(x)N_0(xb/c) - N_0(x)J_0(xb/c)}{1 - (a/b)} \right]^2 - \frac{1}{\sqrt{1 - (2b_0/\lambda)^2}} \left(\frac{2b_0}{\pi d} \sin \frac{\pi d}{b_0} \right)^2$$

$$x = \frac{\pi\gamma_1}{1 - (a/c)} = \frac{c}{a} x_{01}$$

is the root of

$$J_0(x)N_0\left(\frac{xa}{c}\right) - N_0(x)J_0\left(\frac{xa}{c}\right) = 0$$

The second step discontinuity is because of the transition of the characteristic impedance from Z_1 to Z_L , which is a junction of two coaxial guides of different inner but equal

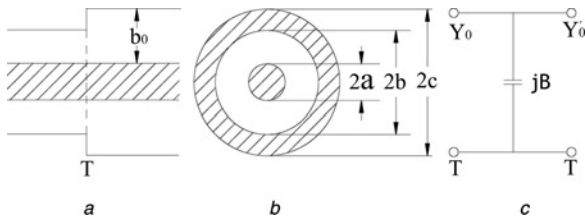


Figure 3 Structure of outer step discontinuity and its equivalent circuit

- a Side view
- b Cross-sectional view
- c Equivalent circuit

outer radii. Fig. 4 shows the structure and the equivalent circuit of the inner step discontinuity. The parameters of the equivalent circuit at the reference plane *T* are given by

$$\frac{Y'_0}{Y_0} = \frac{\ln(c/a)}{\ln(c/b)} \tag{3}$$

$$\frac{B}{Y_0} = \text{same as (2)}$$

where

$$\alpha = 1 - \delta = \frac{c-b}{c-a}, \quad b_0 = c - a, \quad A_1 = \frac{b \ln(c/a)}{a(c/a) - 1} \left[\frac{(c/b) - 1}{\ln(c/b)} \right]^2$$

and

$$A_2 = \frac{\pi^2(a/b)}{\gamma_1 \sqrt{1 - (2b_0/\gamma_1\lambda)^2}} \frac{(c/a) - 1}{[J_0^2(x)/J_0^2(xc/a)] - 1} \times \left[\frac{J_0(x)N_0(xb/a) - N_0(x)J_0(xb/a)}{(c/b) - 1} \right]^2 - \frac{1}{\sqrt{1 - (2b_0/\lambda)^2}} \left(\frac{2b_0}{\pi d} \sin \frac{\pi d}{b_0} \right)^2$$

$$x = \frac{\pi\gamma_1}{(c/a) - 1} = x_{01}$$

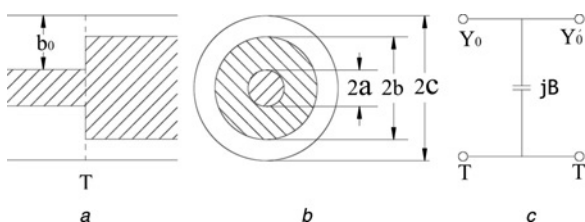


Figure 4 Structure of inner step discontinuity and its equivalent circuit

- a Side view
- b Cross-sectional view
- c Equivalent circuit

is the first non-vanishing root of

$$J_0(x)N_0\left(\frac{xc}{a}\right) - N_0(x)J_0\left(\frac{xc}{a}\right) = 0$$

The parameters of the equivalent circuit of the two step discontinuities can be obtained from (1) to (3). Each of the two step discontinuities can also be modelled as a discontinuity capacitance reactance. Thus, the overall equivalent circuit model of the stepped impedance transformer can be developed as shown in Fig. 5. The model consists of two discontinuities in capacitance and sections of coaxial waveguides represented by transmission lines. In the model, the lengths of the coaxial waveguide corresponding to characteristic impedance Z_0 , Z_1 and Z_L are L_0 , L and L_1 , respectively. Z_R is the impedance of the microstrip probe array, including the impedance of the back-short wall placed by a distance of L_2 from the array. According to the transmission line theory, we have

$$Z_{in3} = Z_L \frac{Z_R + jZ_L \tan \beta L_1}{Z_L + jZ_R \tan \beta L_1} \tag{4}$$

$$Z_{in2} = \frac{Z_{in3}}{1 + jB_2 Z_{in3}} \tag{5}$$

$$Z_{in1} = Z_1 \frac{Z_{in2} + jZ_1 \tan \beta L}{Z_1 + jZ_{in2} \tan \beta L} \tag{6}$$

$$Z_{in0} = \frac{Z_{in1}}{1 + jB_1 Z_{in1}} \tag{7}$$

It is obvious that Z_{in0} can be determined from (4) to (7). If L_0 is chosen to be $n\lambda/2$, then the input impedance is given by $Z_{in} = Z_{in0}$. Using this equivalent model, the input reflection coefficient is given as

$$\Gamma_{in} = \frac{Z_{in} - Z_0}{Z_{in} + Z_0} = \frac{Z_{in0} - Z_0}{Z_{in0} + Z_0} = \frac{Z_{in1} - Z_0 - jB_1 Z_{in1} Z_0}{Z_{in1} + Z_0 + jB_1 Z_{in1} Z_0} \tag{8}$$

Using (1)–(8), the parameters of the overall equivalent circuit model of the coaxial stepped impedance transformer are determined. Conversely, when the value of Γ_{in} is specified, the parameters of the model can also be inverted.

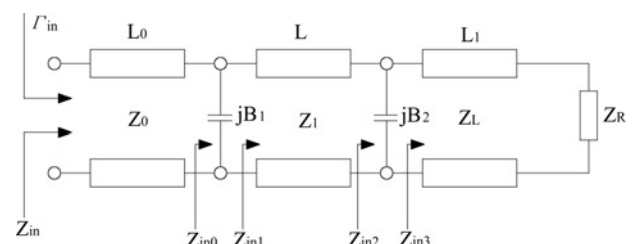


Figure 5 Overall equivalent circuit model of the coaxial stepped impedance transformer

The susceptances of B_1 and B_2 shown in Fig. 5 for the step discontinuities have been calculated using (1)–(3), as shown in Fig. 6. It is obvious that the results of B_1 vary quickly with the outer radius R , whereas the results of B_2 vary slightly with the outer radius R .

2.3 Design and construction of the four-way divider/combiner

By treating the N -way oversized coaxial waveguide power divider as the simplified model [17], the design is reduced to solving a single waveguide to microstrip transition. This design method becomes important when using the full-wave analysis techniques to solve electrically large three-dimensional problems.

In terms of [17], if the divider/combiner consists of a large number of probes, the rectangular waveguide [with perfect magnetic conductor (PMC) side walls] approximation can be used. Otherwise, only sectoral waveguide (with PMC side walls) approximation can be used. For a four-way coaxial waveguide power divider/combiner, the sectoral waveguide approximation is probably valid. Thus, this four-way power divider can be viewed as a structure composed of four identical sectoral waveguides separated by PMC side walls.

A single waveguide-to-microstrip transition is shown in Fig. 7. The sectoral waveguide comprising of a microstrip probe (with PMC side walls and PEC inner and outer walls) is used. There is a transformer between microstrip line and microstrip probe so that the microstrip probe matches to a $50\ \Omega$ microstrip line. The design is then reduced to solving for input match at the waveguide port and output match at the microstrip line port. The

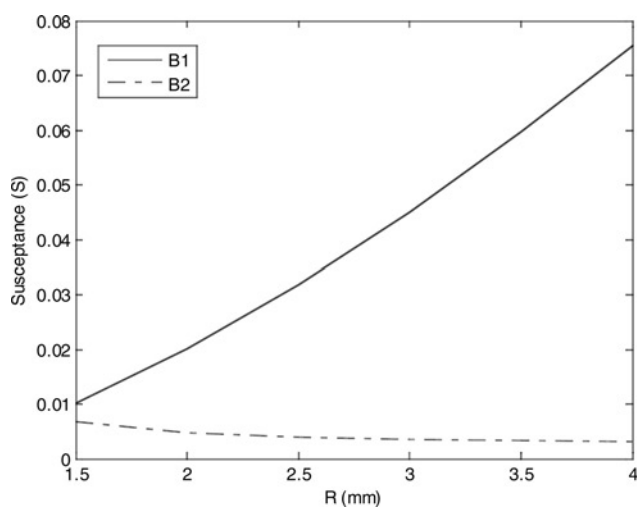


Figure 6 Calculated susceptances of B_1 and B_2 for the step discontinuities

The other dimensions used in the calculations are as follows: $r_1 = 0.3175\ \text{mm}$, $r_2 = 0.71\ \text{mm}$ and $r_3 = 1\ \text{mm}$

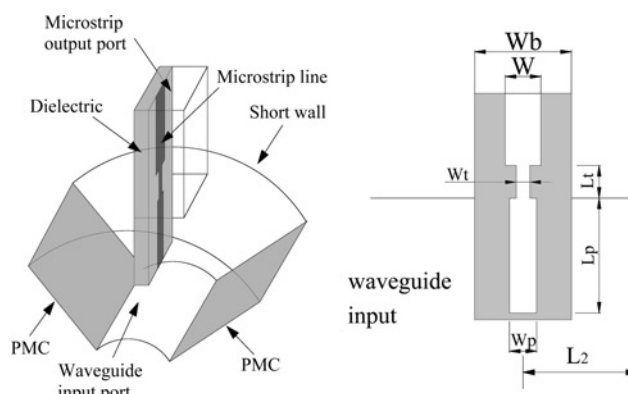


Figure 7 Single waveguide-to-microstrip transition

transition including the short wall was simulated with Ansoft-HFSS.

During the design phase, the probe length L_p , probe width W_p , transformer length L_t , transformer width W_t and the length between the waveguide short wall and the microstrip probe L_2 are adjusted to obtain the desired operation frequency and bandwidth. A transformer of $90\ \Omega$ impedance is used instead of $50\ \Omega$ microstrip lines in order to obtain proper match between the probe and the microstrip line. At $35\ \text{GHz}$, the microstrip probe length is optimised to be approximately $0.2\ \lambda_g$ because of the effective air–dielectric constant at the coaxial waveguide.

Fig. 8a shows the frequency response of the simulated input return loss for different probe lengths L_p and Fig. 8b shows the frequency response for different lengths L_2 between the waveguide short wall and the microstrip probe. Comparing Fig. 8a with Fig. 8b, we can see that the input return loss is more sensitive to L_p than to L_2 .

A four-way oversized coaxial waveguide power divider is designed by expanding the single waveguide-to-microstrip transition. The power dividing structure is simulated using Ansoft-HFSS. Dielectric and conductor losses are included in the simulation. In order to evaluate the performance of the designed power divider, the output power of the coaxial waveguide power divider is recombined through an identical coaxial circuit structure. The simulated frequency response of the passive power dividing/combining structure is shown in Fig. 9. The predicted insertion loss is less than $0.2\ \text{dB}$ across the entire Ka-band except for the range from 39 to $40\ \text{GHz}$, whereas the bandwidth of $20\ \text{dB}$ input return loss is approximately $12\ \text{GHz}$.

3 Experiment and results

A passive four-way oversized coaxial waveguide spatial combiner is built by placing two identical circuits back to back based on the above design. The microstrip probe arrays have been inserted inside the oversized coaxial waveguide at the designed locations. The microstrip circuit board has

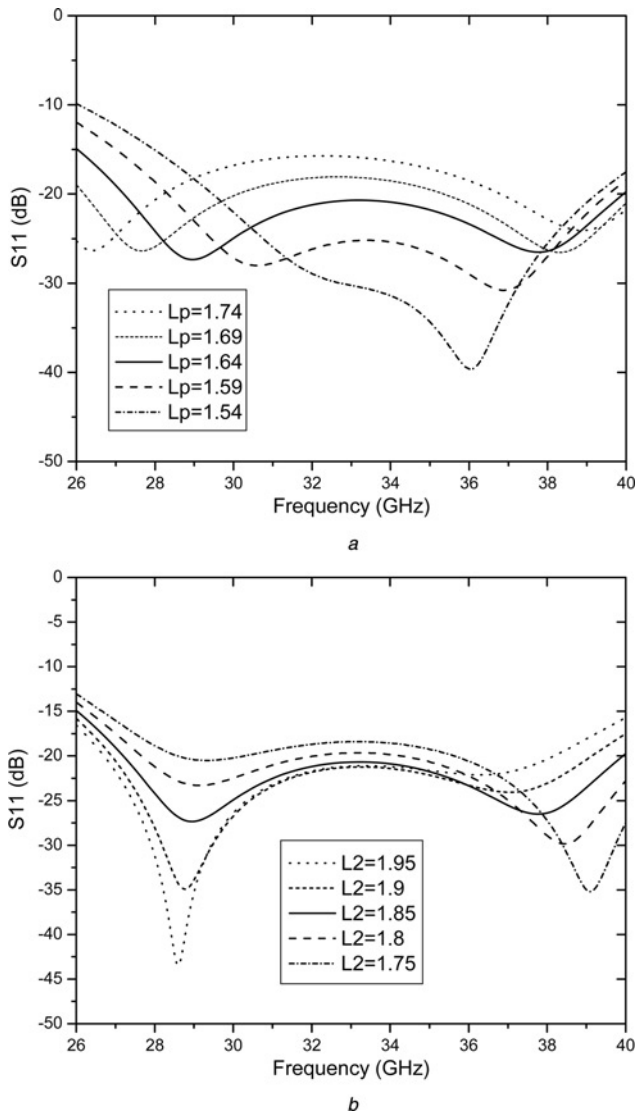


Figure 8 Simulation results of the power divider
The other dimensions used in the simulation are the same as in Table 1

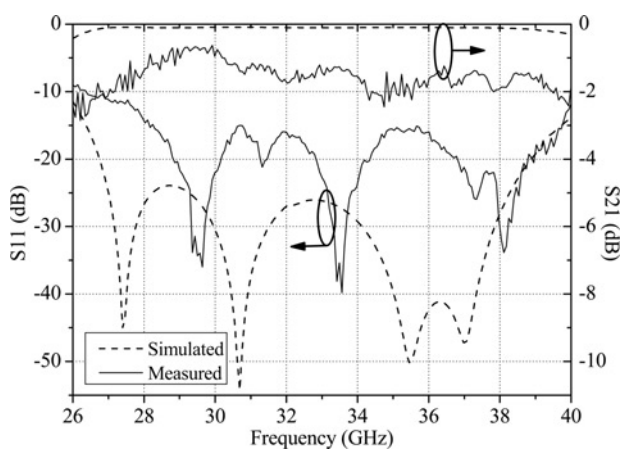


Figure 9 Simulated and measured input return and insertion losses of the passive coaxial waveguide spatial combiner

Table 1 Dimensions of the passive coaxial combiner in mm

Dimensions	Values (mm)
r_1	0.3175
r_2	0.71
r_3	1
R	3.05
L	0.65
L_1	2.15
L_2	1.85
W	0.76
W_t	0.3
W_p	0.58
W_b	3
L_t	0.55
L_p	1.64

been fabricated on a 0.254 mm thick Roger’s 5880 RT/Duroid substrate ($\epsilon_r = 2.2$). The passive combiner is terminated by type-K connectors available commercially. The purpose of using an optimised coaxial stepped impedance transformer is to make sure that the oversized coaxial waveguide matches the 50 Ω input and output lines. The values of the susceptance B_1 and B_2 for the design frequency 35 GHz are 0.0464 (Ω^{-1}) and 0.0034 S, respectively. The final dimensions of the passive four-way coaxial waveguide combiner are listed in Table 1 (as illustrated in Figs. 2 and 7). The overview photograph of the passive four-way coaxial waveguide power dividing/combining system is shown in Fig. 10a. Fig. 10b shows the inside view of the passive combiner system.

The performance of the overall passive system, which includes coaxial stepped impedance transformers, a divider and a combiner, is shown in Fig. 9. The measured

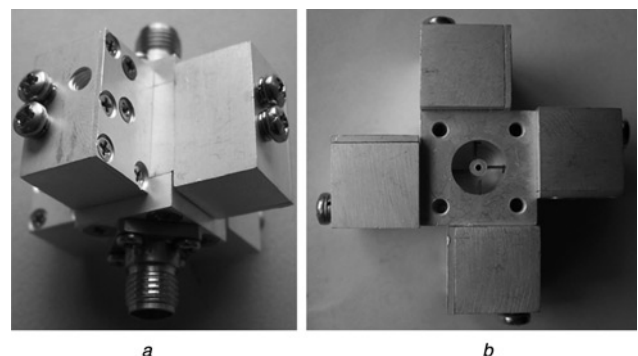


Figure 10 Photograph of the passive spatial combiner
a Overview of the coaxial combiner
b Inside view

insertion loss of the passive system is less than 2.5 dB and the return loss is about 10 dB over the entire Ka-band frequency range (26.5–40 GHz). The measured minimum insertion loss is approximately 0.7 dB and the return loss is smaller than –30 dB at about 29.5 GHz.

The measured results agree qualitatively well with the simulated results, although the maximum return loss and the maximum insertion loss are somewhat higher in the passband. There is evidence of some mismatch at the interface to the type-K connector, leading to the rapid undulations in the frequency response. We attribute the latter to a poor electrical connection between the type-K connector and the centre conductor of the coaxial stepped impedance transformers. The higher insertion loss in the measured response comes mostly from the dielectric loss, insert loss of type-K connectors and imprecision in assembly, which can introduce a loss of more than 1 dB at the higher band.

4 Conclusions

A new oversized coaxial waveguide power combining structure applicable to millimetre-wave applications has been developed. A design procedure is established for coaxial stepped impedance transformer, providing a broadband impedance match between the 50 Ω input coaxial line and the oversized coaxial waveguide. The susceptances of the step discontinuities have been calculated. The trends in the impedance match when the dimensions of the power divider are changed have also been analysed. The results show that the input return loss is more sensitive to L_p than to L_2 . A passive four-way coaxial waveguide power dividing/combining system is designed and fabricated. The input return loss is about 10 dB over the entire Ka-band frequency range (26.5–40 GHz). Very low loss (approximately 0.7 dB) and broadband characteristics have been achieved. These features can make this passive combiner system a good candidate for broadband and efficient power dividing/combining circuits in millimetre-wave communication systems.

5 Acknowledgments

This research was supported in part by the national defence research foundation of China, Youth Science & Technology Foundation of the University of Electronic Science and Technology of China (JX0711) and Montana Tech faculty seed grant.

6 References

[1] FATHY A.E., LEE S.-W., KALOKITIS D.: 'A simplified design approach for radial power combiners', *IEEE Trans. Microw. Theory Tech.*, 2006, **54**, (1), pp. 247–255

[2] SONG K., FAN Y., ZHANG Y.: 'Radial cavity power divider based on substrate integrated waveguide technology', *IEE Electron. Lett.*, 2006, **42**, (19), pp. 1100–1101

[3] YONGSHIK L., EAST J.R., KATEHI L.P.B.: 'Micromachined millimeter-wave module for power combining', *IEEE MTT-S Int. Microw. Symp. Dig.*, 2004, **1**, pp. 349–352

[4] ORTIZ S., HUBERT J., MIRTH L., ET AL.: 'A high-power Ka-band quasi-optical amplifier array', *IEEE Trans. Microw. Theory Tech.*, 2002, **50**, (2), pp. 487–494

[5] AOKI I., KEE S.D., RUTLEDGE D.B., HAJIMIRI A.: 'Distributed active transformer—a new power-combining and impedance-transformation technique', *IEEE Trans. Microw. Theory Tech.*, 2002, **50**, (2), pp. 316–330

[6] DELISIO M.P., YORK R.A.: 'Quasi-optical and spatial power combining', *IEEE Trans. Microw. Theory Tech.*, 2002, **50**, (3), pp. 929–936

[7] CHANG K., SUN C.: 'Millimeter-wave power-combining techniques', *IEEE Trans. Microw. Theory Tech.*, 1983, **MTT-31**, (2), pp. 91–107

[8] BELAID M., MARTINEZ R., WU K.: 'A mode transformer using fin-line array for spatial power-combiner applications', *IEEE Trans. Microw. Theory Tech.*, 2004, **52**, (4), pp. 1191–1198

[9] BECKER J.P., OUDGHIRI A.M.: 'A planar probe double ladder waveguide power divider', *IEEE Microw. Wirel. Compon. Lett.*, 2005, **15**, (3), pp. 168–170

[10] JIANG X., ORTIZ S.C., MORTAZAWI A.: 'A novel Ka-band 1 to 8 power divider/combiner', *IEEE MTT-S Int. Microw. Symp. Dig.*, 2001, **1**, pp. 35–38

[11] JEONG J., KWON Y., LEE S., CHEON C., SOVERO E.A.: '1.6- and 3.3-W power-amplifier modules at 24 GHz using waveguide-based power-combining structures', *IEEE Trans. Microw. Theory Tech.*, 2000, **48**, (12), pp. 2700–2708

[12] JIANG X., ORTIZ S.C., MORTAZAWI A.: 'A Ka-band power amplifier based on the traveling-wave power-dividing/combining slotted-waveguide circuit', *IEEE Trans. Microw. Theory Tech.*, 2004, **52**, (2), pp. 633–639

[13] JIA P.C., LIU Y., CHEN L.Y., YORK R.A.: 'Analysis of a passive spatial combiner using tapered slotline array in oversized coaxial waveguide', *IEEE MTT-S Int. Microw. Symp. Dig.*, 2000, pp. 1933–1936

[14] JIA P.C., CHEN L.Y., ALEXANIAN A., YORK R.A.: 'Multioctave spatial power combining in oversized coaxial waveguide', *IEEE Trans. Microw. Theory Tech.*, 2002, **50**, (5), pp. 1355–1360

[15] JIA P.C., CHEN L.Y., ALEXANIAN A., *ET AL.*: 'Broad-band high-power amplifier using spatial power-combining technique', *IEEE Trans. Microw. Theory Tech.*, 2003, **51**, (12), pp. 2469–2475

[16] ALEXANIAN A., YORK R.A.: 'Broadband waveguide-based spatial combiner', *IEEE MTT-S Int. Microw. Symp. Dig.*, 1997, **3**, pp. 1139–1142

[17] SONG K., FAN Y., ZHANG Y.: 'Investigation of a power divider using a coaxial probe array in a coaxial waveguide', *IEE Proc. Microw. Antennas Propag.*, 2007, **1**, (4), pp. 900–903

[18] MARCUVITZ N.: 'Waveguide handbook' (McGraw-Hill, New York, 1951)